ORIGINAL ARTICLE

Asian Herpetological Research 2020, 11(4): 312–319
DOI: 10.16373/j.cnki.ahr.200001

Toad-headed Lizard *Phrynocephalus forsythii* (Squamata, Agamidae) as a Potential Ring Species Inferred from Population Genetic Differentiation

Yue QI[#], Li DING[#], Yangyang ZHAO, Chenkai NIU, Xiaoning WANG and Wei ZHAO[*]

Gansu Key Laboratory of Biomonitoring and Bioremediation for Environmental Pollution, School of Life Sciences, Lanzhou University, Lanzhou 730000, China

Abstract Speciation has never been directly observed in nature because it is a lengthy phenomenon. Although rare, ring species are an optimal natural example of speciation and can be identified through the assessment of the geographical conditions of their potential habitat. *Phrynocephalus forsythii* is endemic to the Tarim Basin, which comprises the Taklamakan Desert and surrounded by mountains on three sides. This study aimed to determine whether *P. forsythii* had a ring-species-like divergence pattern through the characterization of the genetic features of 17 populations covering the major distribution of this species. Species distribution modelling revealed that *P. forsythii* had a continuous circular distribution around the Tarim Basin. Gene flow was observed in most adjacent populations except for two terminal populations of the ring, which exhibit the highest differentiation. Genetic distance and geographic distance were significantly correlated, indicating that the observed differentiation resulted from genetic variation gradually accumulating during population dispersion. Although our results do not definitively indicate that *P. forsythii* is a ring species, our results indicate a ring-shaped diversification. This phenomenon elucidates the potential mechanism underlying speciation in the presence of gene flow, providing insight into this evolutionary process.

Keywords continuous variation, gene flow, *Phrynocephalus forsythii*, ring species, Tarim Basin

[#] Both authors contribute equally to this work.
[*] Corresponding author: Dr. Wei ZHAO, from School of Life Sciences, Lanzhou University, China, with his research mainly focusing on evolution and biogeography of reptiles.
E-mail: zhaowei@lzu.edu.cn
Received: 6 January 2020 Accepted: 24 April 2020

1. Introduction

Ring species are among the best natural illustrations of speciation (Kuchta, 2016). Understanding speciation is a fundamental biological problem. During classical ecological speciation, population fragmentation yields new species from geographically isolated populations of the same ancestral species (Dieckmann and Doebeli, 1999; Schluter, 2001). However, speciation is gradual phenomenon and thus has not been observed directly in nature. Instead, assessment of ring species may provide insights into speciation, a chain of intergrading populations that encircle a barrier, with terminal forms coexisting without interbreeding (Mayr, 1942). Ring species represent a phenomenon wherein reproductive isolation can be produced in the presence of continuous gene flow and genetic variation (Irwin and Wake, 2016; Hey *et al.*, 2005). In brief, ring species help us to understand how intraspecific geographical variation generates species-level divergence and are integral to speciation studies (Irwin *et al.*, 2001; Cacho and Baum, 2012).

Considering their evolutionary significance, numerous studies have attempted to identify ring species. Ideally, the criteria that should be met are: circular distribution, gene flow, and reproductive isolation (Joseph *et al.*, 2008; Qiao *et al.*, 2018). A typical ring species must first meet the requirements in terms of distribution, in that the sub-populations around a barrier are derived from an ancestral population. Such barriers can consist of regions with a slope around them or environmental variations that do not generate a suitable habitat for a specific species (Irwin, 2012; Fuchs *et al.*, 2015; Pereira and Wake, 2015). Nevertheless, gene flow may link the circular chain of populations around barriers. With an increase in the geographical distance around the ring, genetic variation among populations would also gradually accumulate (Alcaide *et al.*, 2014). This accumulation of genetic differences eventually leads to reproductive isolation between the two sub-populations at

the far ends of the chain (terminal populations) (Dufresnes *et al.*, 2016; Irwin *et al.*, 2001).

A promising candidate for ring species is *Phrynocephalus forsythii*, a lizard endemic to the Tarim Basin (Adler and Zhao, 1993). Surrounded by mountains on three sides, the Tarim Basin also contains the largest shifting-sand desert in central Asia, the Taklamakan Desert (Zheng *et al.*, 2009). Furthermore, the outer circle of the basin is surrounded by an oasis. These environmental conditions provide an ideal environment for the evolution of ring-like species. *P. forsythii* is distributed in the oasis around the Tarim Basin (Figure 1) and prefers a habitat with dwarf shrubs (Zhang *et al.*, 2010), a humid environment, and a lower ambient temperature (Qi *et al.*, 2019). Previous studies on the phylogeographic structure of *P. forsythii* have reported that two adjacent populations (MF and RQ) belong to different lineages, thereby indicating the potential for reproductive isolation between these two adjacent populations (Qi *et al.*, unpublished data). These genetic and distribution characteristics render *P. forsythii* an excellent candidacy for the assessment of ring species. Therefore, this study aimed to determine whether *P. forsythii* had a ring species-like divergence pattern by characterization of its genetic structure and gene flow.

2. Materials and Methods

2.1. Ethics statement All experiments were approved by and were in accordance with the Ethics Committee of the School of Life Sciences, Lanzhou University.

2.2. Sampling and species distribution modelling This study included 210 specimens from 17 localities, encompassing majority of the distribution range of *P. forsythii* (Table S1 and Figure 1). Field identification was based on external morphological characteristics (Zhu *et al.*, 1999).

The current potential of the species and suitable range were estimated using Maxent version 3.3.3 (Elith *et al.*, 2011; Phillips *et al.*, 2006). Field records and the literature yielded 29 *P. forsythii* occurrences (Zhang *et al.*, 2010) (Table S2). Environmental data included 19 bioclimatic variables from the WorldClim database (http://www.worldclim.org/; Hijmans *et al.*, 2005) (Table S3); spatial resolution was 2.5 arc minute (~4 km). Model complexity was evaluated with "ENMeval" in R 3.6.1 (R Core Team 2017), through the determination of the Maxent-corrected AIC under different parameters. Thirteen variables were included in the final analysis. Species distribution modeling (SDM) was performed using Maxent, with occurrence data randomly segregated into 80% training and 20% testing data. This model used the default convergence threshold, 5,000 maximum iterations, and 10 replicates. An ROC curve close to 1 indicated a better model performance (Phillips *et al.*, 2006).

2.3. Laboratory analyses DNA was extracted from muscle samples, using the TIANamp Genomic DNA Kit (Qiagen, Beijing, China) in accordance with the manufacturer's instructions. Three mitochondrial genes (*ND2, ND4,* and *Cyt-b*) were amplified. Primers were designed using PRIMER 6.0. PCR annealing temperatures are enlisted in Table S4. Sequences were assembled manually using SeqMan 7.1.0 in DNA Star, aligned in BioEdit version 7.1.3.0 (Hall, 1999), and concatenated using Sequence Matrix 1.7.8 (Vaidya *et al.*, 2011) for further analyses. All mitochondrial markers were deposited in the GenBank database (accession nos. MK803503–MK804072 and MN872429–MN872473).

Genomic DNA was incubated at 37℃ with MseI (New England Biolabs, NEB), T4 DNA ligase (NEB), ATP (NEB), and MseI Y adapter N containing barcode, and fragments of 350 bp in size were isolated using a Gel Extraction Kit (Qiagen) in accordance with the manufacturer's instructions. Thereafter, the genomic DNA of the samples was amplified via PCR, and the constructed libraries were sequenced using the Illumina HiSeq sequencer with a 150-bp paired-end sequencing strategy. The sequencing quality requirement for most bases was set at >Q20. Raw reads were filtered to eliminate reads containing adapters or reads of low quality, such that downstream analyses were then based on clean reads. The whole-genome sequencing data of *Phrynocephalus vlangalii* (GWHAAFC00000000) were used as the reference genome. Sequencing data were then aligned with the reference sequence using the BWA software (parameters: mem -t 4 -k 32 -M) (Li and Durbin, 2009). SAMTOOLS (mpileup -m 2 -F 0.002 -d 1000) was used to detect SNP of individuals (Li *et al.*, 2009).

2.4. Data analysis

Phylogeographic analysis Bayesian analyses were performed using AIC in MrBayes 3.2.6 (Huelsenbeck and Ronquist, 2001) with the GTR+I+G model selected by MrModeltest 2.3 (Nylander, 2004). For the Bayesian analysis, 20 million generations with the Markov Chain Monte Carlo (MCMC) simulations were performed until the average SD of split frequencies decreased to <0.01; the initial 25% were discarded as burn-in frequencies. Simulations used the default model parameters starting from a random tree. Outgroups were *P. axillaris* and *P. mystaceus*. All tree files were visualized using Figtree 1.3.1.

Population genetic analysis Pairwise F_{ST} (between-population differentiation) and isolation-by-distance were estimated using Arlequin 3.5 (Excoffier *et al.*, 2005). In this program, genetic distance is determined as $F_{ST}/(1–F_{ST})$. Straight-line geographic distances and ring distances among the sites were used to analyze isolation by distance. Ring distances were determined as geographic distances, assuming that dispersal routes follow ring distribution rather than straight lines across

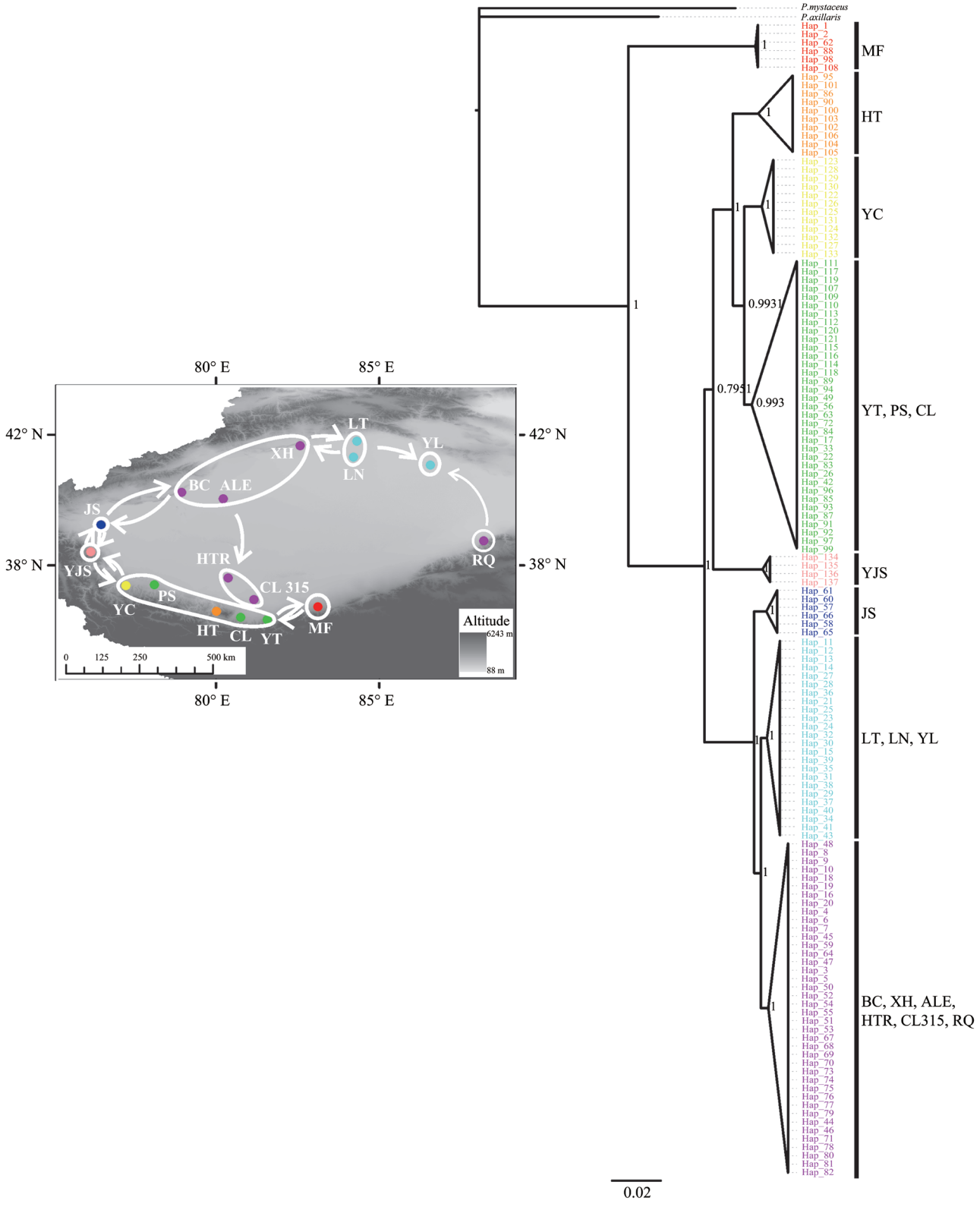

Figure 1 Geographical features and locations of sampling sites. For locality names, see Table S1. Dot color corresponds to population structure derived from the phylogenetic tree. Arrows represent direction of gene flow. All populations were divided into nine groups based on phylogeny: Group1, MF; Group 2, HT, YT, YC, PS, CL; Group 3, YJS; Group 4, BC, XH, ALE; Group 5, LN, LT; Group 6, JS; Group 7, YL; Group 8, RQ; Group 9, HTR, CL315.

the uninhabitable desert. Phylogeographic analysis suggested a genetic "gap" between populations RQ and MF. Thus, MF was selected as the origin and RQ as the terminus to determine the ring distance among all populations (Qi *et al.*, unpublished data). Correlations between genetic and geographic distances were determined using a Mantel test with 1000 permutations and Arlequin 3.5.

Gene flow between populations Using maximum-likelihood migration rates, between-population gene flow was estimated using Migrate 3.7.2 (Beerli, 1997). This approach uses MCMC searches to account for unequally effective population sizes and asymmetrical gene flow (Beerli and Felsenstein, 1999). As in some lineages, populations were not continuously distributed geographically; rather, they were divided by populations from other lineages. The present grouping strategy was thus determined through the phylogenetic structure and geographic distribution of all populations. All populations were divided into nine groups, and gene flow was determined (Figure 1). Initial values of effective population sizes and gene flow were estimated from F_{ST}. The analysis involved 10 short chains (500 trees used out of 10,000 sampled) and three long chains (5000 trees out of 100,000). Results from 10 runs were averaged and 95% confidence intervals were summarized.

Furthermore, population divergence and mixing patterns were inferred from *P. forsythii* SNP data in TreeMix 1.13 (Pickrell and Pritchard, 2012; Wang *et al.*, 2015). Custom Perl scripts were used to enumerate the variation of all individuals into populations. Thereafter, a maximum-likelihood tree was estimated and migration events were superimposed over it, such that the tree with the added migration episodes accounts for a greater proportion of the overall genetic variance. We allowed for 10–11 migration events. The final results were visualized using R 3.6.1.

To better estimate historic gene flow between populations from MF and RQ, we used IMa2 based on the IM model (Hey, 2010b) with mtDNA data. In this analysis, demographic parameters, including divergence time (*t*), effective population size of each extant population (*q0* and *q1*) and the ancestor (*q2*), and migration rates (*m0* and *m1*) between two groups, scaled by the mutation rate, were estimated. The maximum priors for the parameters used for IMa analyses were $t = 5$, $q = 10$, and $m = 100$. In the simulations, we conducted each IMa simulation for 100000 steps with a burn-in of 100000 steps.

3. Results

3.1. Prediction of species distribution SDM analysis revealed that this model was a good fit with an AUC of >0.9. The most suitable habitats for *P. forsythii* were around the Basin (Figure 2), with the western region being more habitable than the eastern region. Finally, we observed a gap in the inhabitable region along the eastern region.

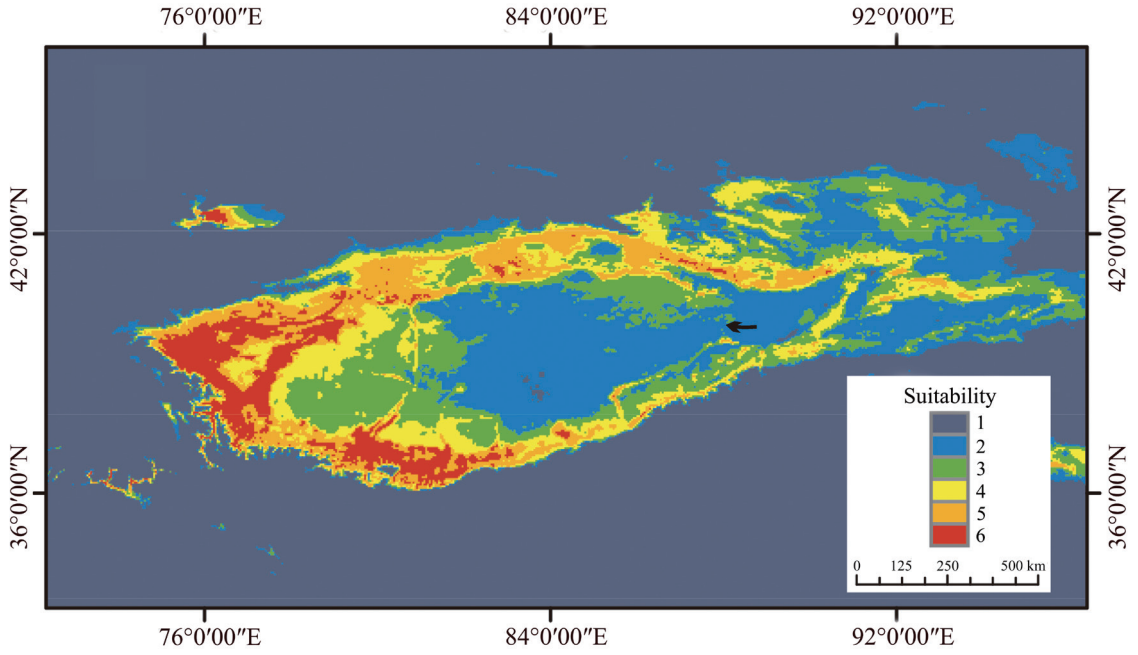

Figure 2 Distribution models for *Phrynocephalus forsythii*. Warmer colors represent greater likelihood of occurrence (red = 6, blue = 1). Scale bar indicates occurrence probability. The arrow points represent the distributed gap points.

3.2. Sequence data

Mitochondrial DNA We obtained 210 mitochondrial gene sequences with an average length of 3538 bp and identified 137 haplotypes (Table S1). The nucleotide composition was as follows: A = 0.351, C = 0.270, G = 0.132, and T = 0.247.

Single-nucleotide polymorphisms Sequencing of the GBS library comprising 146 samples yielded 786522636 clean reads with an average of 5387141 reads per sample. We successfully mapped 755235460 reads, and the average mapping rate was 96.05%. Finally, 544574 SNPs were filtered from 11710171 raw SNPs.

3.3. Population genetic analysis

Phylogeographic analyses Haplotypes derived from the Bayesian analysis of the 17 populations formed three distinct clusters: first, the population from Minfeng (the Minfeng Group), was separated from all other populations, and the other populations were grouped into two clades with non-overlapping distribution: six populations located to the north of the Tarim Basin formed a large distinctive group (the northern group: JS, LT, LN, YL, BC, XH, ALE, HTR, CL315 and RQ), and nine populations located in the south of Tarim Basin formed a second distinctive group (the southern group: HT, YC, YT, PS, CL and YJS) (Figure 1).

Population analyses Pairwise F_{ST} differed significantly from zero ($P < 0.001$) (Table S5). Pairwise F_{ST} was the greatest between MF and RQ despite their adjacent distribution. Genetic distance and ring distances were positively correlated (Mantel's $r = 0.407$, $P < 0.001$), consistent with a pattern of isolation by distance around the ring (Figure 3). Furthermore, the correlation between straight-line geographic distances and genetic distance was significant (Mantel's $r = 0.243$, $P = 0.02$) (Figure 3).

Gene flow Most adjacent groups exhibited gene flow except for groups 1 (MF) and 8 (RQ) (Figure 1; Table S6). Concurrent with the mtDNA results, predicted migration events revealed frequent gene exchange between adjacent populations (Figure 1). Integrating Migrate and TreeMix data revealed a gene-flow model of ring species, thereby indicating that almost all adjacent populations displayed gene flow except for MF and RQ. Furthermore, historic gene flow analysis based on IMa2 indicated no gene flow between MF and RQ. The migration rates (2NM) from MF to RQ and vice versa were 0.05062 and 0.04556, respectively. However, gene flow was confirmed only when 2NM values were significant in an LLR test ($P < 0.05$ or less) (Hey, 2010a; Nielsen and Wakeley, 2001). The present results showed that the migration rate (2NM) from MF to RQ and vice versa was not significant. Therefore, we considered that there was no gene flow between MF and RQ (Table 1).

4. Discussion

Our results show that *P. forsythii* conforms to the ring species model. First, the *P. forsythii* recorded distribution and SDM data indicated that it had a continuous circular distribution around the Tarim Basin. Second, populations of MF and RQ are linked by a chain of interbreeding populations wrapping around the Tarim Basin. Finally, these two terminal populations, MF and RQ, are genetically distinct.

The distribution of *P. forsythii* populations along the ring structured in a manner similar to that of the ring species model (Alcaide *et al.*, 2014). Although SDM implied the presence of a gap in the eastern region of the basin, the distribution between MF and RQ was continuous. Therefore, we consider

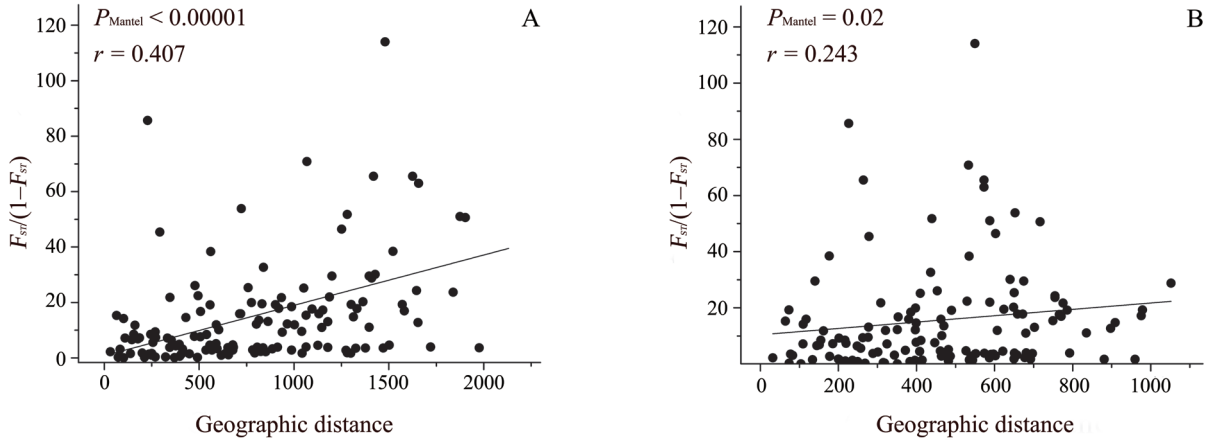

Figure 3 Genetic distance (calculated from mtDNA) increases with geographic distance around the ring. A: Correlation when "ring distances" are used. B: Correlation when straight geographic distances between sites are used. We assumed no direct gene flow between MF and RQ or across the center of the ring. Ring distances approximate potential gene flow between populations around the Tarim Basin.

the *P. forsythii* distribution to be ring-shaped. Such a ring-shaped structure may result from the development of a dense hydrological network around the Tarim Basin and the expansion of the Taklimakan desert. Phylogeographic analysis revealed that after populations first differentiated from MF, the western populations (e.g., JS and YJS) diverged from the northern and southern groups, respectively. Accordingly, we speculated that *P. forsythii* originated from the northern side of the Kunlun Mountains. Thereafter, the remaining populations dispersed northward and eastward along the edge of Tarim Basin. The divergence time of the northern group and the southern group coincide with the formation of rivers and oases around the Tarim Basin and the expansion of the Taklimakan (Qi *et al.*, unpublished data). These geological features probably explain the ring-shaped distribution structure observed herein in *P. forsythii*. Furthermore, the Taklimakan Desert is a barrier similar to that observed with *Phylloscopus trochiloides*, a classic ring species in Asia, which is isolated by a large treeless gap (Irwin *et al.*, 2001). We thus speculate that after MF initially differentiated, the remaining *P. forsythii* populations expanded along the basin.

Our Migrate and TreeMix results provided the strongest evidence for a gene flow pattern that supported *P. forsythii* as a ring species. In particular, we found no break in gene flow throughout the ring of populations, except between MF and RQ (Figures 1 and 4). This generally uninterrupted gene flow is due to short-distance dispersal in a continuously distributed species (Joseph *et al.*, 2008). Our previous studies on *P. forsythii* population history indicate that they have not experienced rapid expansion (Qi *et al.*, unpublished data). Therefore, we can speculate that, after initially differentiating from the northern and southern groups, the westernmost populations gradually spread eastward. Therefore, the short-distance dispersal was probably a gradual process among *P. forsythii* that eventually led to gene flow between adjacent populations (Slatkin *et al.*, 1993).

Finally, our F_{ST}, migration and IMa analyses among populations consistently displayed restricted gene flow among terminal populations MF and RQ, suggesting some degree of reproductive isolation (Figure 1 and Table S5). As expected in

Table 1 Maximum-likelihood estimates (MLE) and 90% highest posterior density (HPD) intervals of demographic parameters from IMa multilocus analyses

	t0	*q0*	*q1*	*q2*	*2N0M0*	*2N1M1*
MLEs	4.915	1.64	1.359	1.987	0.05062	0.04556
HPD95Lo	4.747	1.101	0.663	1.959	0	0
HPD95Hi	4.997	1.999	1.999	1.999	0.1681	0.1411

t0: Time since major lineage divergence; *q0, q1, q2*: Effective population size of MF, RQ, and ancestral population; *2N0M0*: Population migration rate from the RQ to MF; *2N1M1*: Population migration rate from MF to RQ.

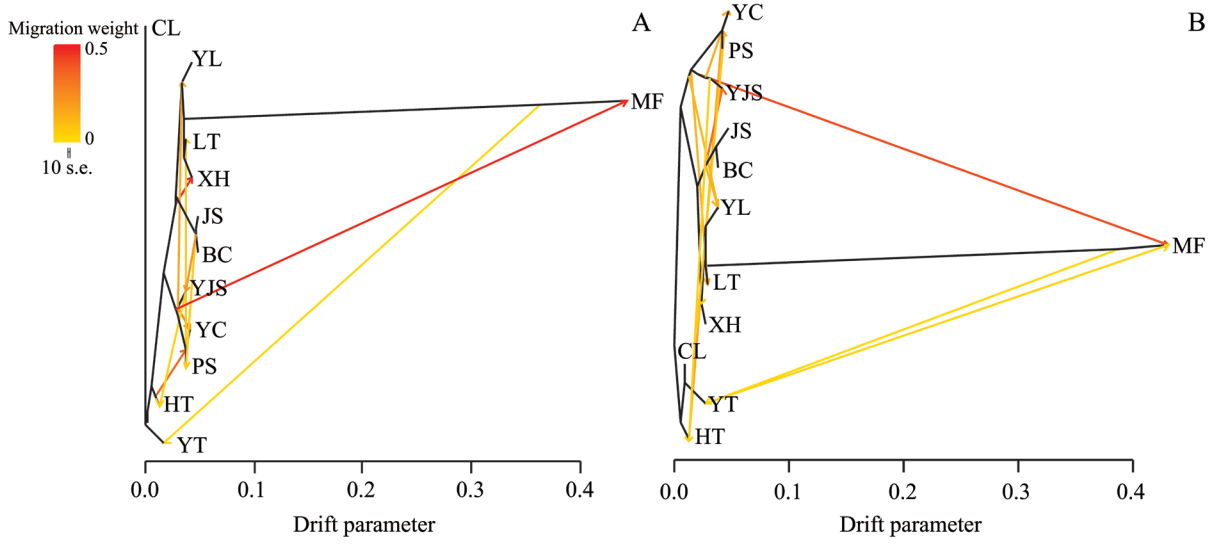

Figure 4 Inferred maximum-likelihood trees of mixture events. Abbreviations are the same as in Table S1. Graphs inferred for all populations, allowing ten (A) and eleven (B) migration events. Migration arrows are colored in accordance with their weight.

a ring species, MF and RQ are associated with populations within the chain. Although these other populations exhibit gene flow, we could also detect gradual and continuous genetic variation among them. The finding of a markedly strong correlation between genetic distance and geographic distance (Figure 3) indicates that variation in genomic composition will increase as populations move further away from each other during species dispersal. Adjacent populations would therefore possess very few genetic differences, whereas distant populations will accumulate enough differences, resulting in reproductive isolation (Slatkin, 1993). Previous studies have similarly suggested that long-distance dispersal in a continuously distributed species results in isolation by distance (Irwin *et al.*, 2005).

Owing to the lack of a direct evidence of reproductive isolation, we cannot definitively claim that *P. forsythii* is a ring species (Irwin *et al.*, 2001; Pereira *et al.*, 2011). However, the ring-shaped diversification of *P. forsythii* is notable as a clear manifestation of speciation processes, and we can consider our study populations as intermediate transition species (Niemiller *et al.*, 2008; Nosil, 2008). Environmental changes may interrupt the ring-species model by breaking these populations into two or more species that do not exchange genes (Gavrilets *et al.*, 1998; Doebeli and Dieckmann, 2003). Global warming, a known threat to *P. forsythii* (Sinervo *et al.*, 2018; Qi *et al.*, 2019), may cause the obliteration of some populations and interrupt the chain. Thus, a major challenge for modern evolutionary biology is to develop strategies that can protect the balance between gene flow and isolation mechanisms among potential ring species such as *P. forsythii*. In addition to these long-term implications, our work also deepens our existing understanding of species formation.

Acknowledgements The study was supported by the National Natural Science Foundation of China (No. 31471988 and No. 31200287).

Reference

Adler K., Zhao E. M. 1993. Society for the study of amphibians and reptiles. Amphibia-Reptilia, 16: 423–424

Alcaide M., Scordato E. S. C., Price T. D., Irwin D. E. 2014. Genomic divergence in a ring species complex. Nature, 511: 83–85

Ayala F. J., Fitch W. M. 1997. Genetics and the origin of species: An introduction. P Nat Acad Sci, 94: 7691–7697

Beerli P. 1997. Migrate 0.7: Documentation and program, part of LAMARC. http://evolution.genetics.washington

Beerli P., Felsenstein J. 1999. Maximum-likelihood estimation of migration rates and effective population numbers in two populations using a coalescent approach. Genetics, 152: 763–773

Cacho N. I., Baum D. A. 2012. The Caribbean slipper spurge Euphorbia tithymaloides: The first example of a ring species in plants. P Roy Soc B: Biol Sci, 279: 3377–3383

Dieckmann U., Doebeli M. 1999. On the origin of species by sympatric speciation. Nature, 400: 354–357

Doebeli M., Dieckmann U. 2003. Speciation along environmental gradients. Nature, 421: 259–264

Dufresnes C., Litvinchuk S. N., Leuenberger J., Chali K., Zinenko O. 2016. Evolutionary melting pots: A biodiversity hotspot shaped by ring diversifications around the Black Sea in the Eastern tree frog (*Hyla orientalis*). Mol Ecol, 25: 4285–4300

Elith J., Phillips S. J., Hastie T., Dudík M., Chee Y. E. 2011. A statistical explanation of MaxEnt for ecologists. Divers Distrib, 17: 43–57

Fuchs J., Ericson P. G., Bonillo C., Couloux A., Pasquet E. 2015. The complex phylogeography of the Indo-Malayan Alophoixus bulbuls with the description of a putative new ring species complex. Mol Ecol, 24: 5460–5474

Excoffier L., Laval G., Schneider S. 2005. Arlequin (version 3.0): An integrated software package for population genetics data analysis. Evol Bioinform Online, 1: 47–50

Gavrilets S., Hai L., Vose M. D. 1998. Rapid parapatric speciation on holey adaptive landscapes. P Roy Soc, 265: 1483–1489

Hall T. A. 1999. BioEdit: A user-friendly biological sequence alignment editor and analysis program for Windows 95/98/NT. Nucl Acid Symp Ser, 41: 95–98

Hey J., Fitch W. M., Ayala F. J. 2005. Systematics and the origin of species. P Nat Acad Sci, 102: 6515–6519

Hey J. 2010a. The divergence of chimpanzee species and subspecies as revealed in multipopulation isolation-with-migration analyses. Mol Biol Evol, 27: 921–933

Hey J. 2010b. Isolation with migration models for more than two populations. Mol Biol Evol, 27: 905–920

Hijmans R. J., Cameron S. E., Parra J. L., Jones P. G., Jarvis A. 2005. Very high-resolution interpolated climate surfaces for global land areas. Inter J Clim, 25: 1965–1978

Huelsenbeck J. P., Ronquist F. 2001. MRBAYES: Bayesian inference of phylogenetic trees. Bioinformatics, 17: 754–755

Irwin D. E., Bensch S., Price T. D., 2001. Speciation in a ring. Nature, 409: 333–337

Irwin D. E., Irwin J. H., Price T. D. 2001. Ring species as bridges between microevolution and speciation. Genetica, 112: 223–243

Irwin D. E. 2005. Speciation by distance in a ring species. Science, 307: 414–416

Irwin D. E. 2012. A novel approach for finding ring species: Look for barriers rather than rings. BMC Biology, 10: 21

Irwin D. E., Wake D. B. 2016. Ring species. Encycl Evol Biol, 3: 467–475

Joseph L., Dolman G., Donnellan S., Saint K. M., Berg M. L. 2008. Where and when does a ring start and end? Testing the ring-species hypothesis in a species complex of Australian parrots. P Roy Soc, 275: 2431–2440

Kuchta R., Wake D. B. 2016. Wherefore and whither the ring species? Copeia, 104: 189–201

Li H., Durbin R. 2009. Fast and accurate short read alignment with Burrows-Wheeler transform. Bioinformatics, 25: 1754–1760

Li H., Handsaker B., Wysoker A., Fennell T., Ruan J. 2009. The sequence alignment/map format and SAMtools. Bioinformatics, 25: 2078–2079

Liu J. Q., Qin X. G. 2005. Evolution of the environmental framework

and oasis in the Tarim Basin. Quat Sci, 25: 533–539

Mayr E. 1942. Systematics and the origin of species. P Nat Acad Sci, 102: 6515–6519

Muscarella R., Galante P. J., Soley-Guardia M., Boria R. A., Kass J. M. 2014. ENMeval: An R package for conducting spatially independent evaluations and estimating optimal model complexity for MAXENT ecological niche models. Methods Ecol Evol, 5: 1198–1205

Nielsen R., Wakeley J. 2001. Distinguishing migration from isolation: A Markov chain Monte Carlo approach. Genetics, 158: 885–896

Niemiller M. L., Fitzpatrick B. M., Miller B. T. 2008. Recent divergence-with-gene-flow in Tennessee cave salamanders (Plethodontidae: Gyrinophilus) inferred from gene genealogies. Mol Ecol, 17: 2258–2275

Nosil P. 2008. Speciation with gene flow could be common. Mol Ecol, 17: 2103–2106

Nylander J. A. A. 2004. MrModeltest v2. Program distributed by the author. Evolutionary Biology Centre, Uppsala University.

Pereira R. J., Monahan W. B., Wake D. B. 2011. Predictors for reproductive isolation in a ring species complex following genetic and ecological divergence. BMC Evol Biol, 11: 1–15

Pereira R. J., Wake D. B. 2015. Ring species as demonstrations of the continuum of species formation. Mol Ecol, 24: 5312–5314

Pickrell J. K., Pritchard J. K. 2012. Inference of population splits and mixtures from genome-wide allele frequency data. PLoS Genet, 8: e1002967

Phillips S. J., Anderson R. P., Schapire R. E. 2006. Maximum entropy modeling of species geographic distributions. Ecol Mod, 190: 231–259

Qi Y., Zhao W., Huang Y. J., Wang X. N., Zhao Y. Y. 2019. Correlation between climatic factors and genetic diversity of *Phrynocephalus forsythii*. Asian Herpetol Res, 10(4): 270–275

Qiao L., Wen G. N., Qi Y., Lu B., Hu J. H., Song Z. B., Fu J. Z. 2018. Evolutionary melting pots and reproductive isolation: A ring-shaped diversification of an odorous frog (*Odorrana margaratea*) around the Sichuan Basin. Mol Ecol, 27: 4888–4900

Synes N. W., Osborne P. E. 2011. Choice of predictor variables as a source of uncertainty in continental-scale species distribution modeling under climate change. Glob Ecol Biogeogr, 20: 904–914

Schluter D. 2001. Ecology and the origin of species. Trends Ecol Evol, 16: 372–380

Sun J. M., Liu T. S. 2006. The age of the Taklimakan Desert. Science, 312: 1621–1621

Sun J. M., Liu W. G., Liu Z. H., Deng T., Windley B. F. 2017. Extreme aridification since the beginning of the Pliocene in the Tarim Basin, western China. Palaeogeogr Palaeoclimatol Palaeoecol, 485: 189–200

Sinervo B., Miles D. B., Wu Y. Y., Kirchoff S., Fausto R. 2018. Climate change, thermal niches, extinction risk and maternal-effect rescue of toad-headed lizards, Phrynocephalus, in thermal extremes of the Arabian Peninsula to the Tibetan Plateau. Integrat Zool, 13: 450–470

Slatkin M. 1993. Isolation by distance in equilibrium and non-equilibrium populations. Evolution, 47: 264–279

Team C. R. 2017. R: A language and environment for statistical computing. Vienna, Austria. https://www.R-project.org/

Vaidya G., Lohman D. J., Meier R. 2011. SequenceMatrix: Concatenation software for the fast assembly of multi-gene datasets with character set and codon information. Cladistics, 27: 171–180

Wang M. S., Li Y., Peng M. S., Zhong L., Wang Z. J. 2015. Genomic analyses reveal potential independent adaptation to high altitude in Tibetan chickens. Mole Biol Evol, 7: 1880–1889

Zhang Q., Xia L., He J. B., Wu Y. H., Fu J. Z. 2010. Comparison of phylogeographic structure and population history of two Phrynocephalus species in the Tarim Basin and adjacent areas. Mol Phylogenet Evol, 57: 1091–1104

Zheng H., Jia J. T., Wang K. 2009. Cenozoic sediments in the southern Tarim Basin: Implications for the uplift of northern Tibet and evolution of the Taklimakan Desert. Earth Sci Front, 22: 321–31

Zhu H., Zheng Z., Huang D., Song D., Feng Z. 1999. Fauna Sinica Vol. 2, Reptilia: Squamata, Science Press, Beijing, China (In Chinese)

Handling Editor: Heling Zhao

How to cite this article:

Qi Y., Ding L., Zhao Y. Y., Niu C. K., Wang X. N., Zhao W. Toad-headed Lizard *Phrynocephalus forsythii* (Squamata, Agamidae) as a Potential Ring Species Inferred from Population Genetic Differentiation. Asian Herpetol Res, 2020, 11(4): 312–319. DOI: 10.16373/j.cnki.ahr.200001

Appendix

Table S1 *P. forsythii* samples information in this study.

Sampling site	Sample size	mtDNA		SNP	Sample code	Haplotype code
		number	haplotype	number		
Minfeng (MF)	12	12	6	12	1,2,3,4,5,6,7,8,9,10,11,12	h1,h2,h62,h88,h98,h108
Cele (CL)	16	16	15	16	13,14,15,16,17,18,19, 20,21,22,23,24,25,26	h17,h22,h26,h33,h42, h49,h56,h63,h72,h83,h84
Yutian (YT)	14	14	11	13	27,28,29,30,31,32,33,34, 35,36,37,38,39,40,41,42	h85,h86,h87,h89,h90,h91,h92, h93,h94,h95,h96,h97,h99,h100,h101
Hetian (HT)	11	11	11	-	43,44,45,46,47,48,49, 50,51,52,53,54,55,56	h102,h103,h104,h105,h106
Pishan (PS)	14	14	5	13	58,60,61,62,63,64,65,66, 67,68,69,70,71,72,73,74	h107,h109,h110,h111,h112, h113,h114,h115,h116,h117, h118,h119,h120,h121
Yecheng (YC)	4	4	4	-	76,77,78,79,80,81,82, 83,84,85,86,87,88,89	h122,h123,h124,h125,h126,h127, h128,h129,h130,h131,h132,h133
Yingjisha (YJS)	19	16	14	19	90,91,92,93,94,95,96,97	h134,h135,h136,h137
Bachu (BC)	14	14	12	14	98,99,100,101,102, 103,104,105,106,107,108	h3,h4,h5,h6,h7
Xinhe (XH)	8	8	4	8	109,110,111,113,114,115,116	h8,h9,h10
Luntai (LT)	12	11	8	12	117,118,119,120,121, 122,124,125,126,127	h11,h12,h13,h14,h15
Ruoqiang (RQ)	18	18	11	-	129,131,132,133,134,135,136,138	h16,h18,h19,h20
Yuli (YL)	11	11	5	11	139,140,141,142,143,144,145, 147,149,150,151,152,153,154	h21,h23,h24,h25,h27,h28
Luntainan (LN)	8	7	3	8	156,157,158,159,160,161,162,163, 164,165,166,167,168,171,172,173,174	h29,h30,h31,h32,h34,h35, h36,h37,h38,h39,h40,h41,h43
Alae (ALE)	10	10	5	6	175,176,177,178,179,180,181,182,183, 184,185,186,187,188,189,190,191,192	h44,h45,h46,h47,h48, h50,h51,h52,h53,h54,h55
Jiashi (JS)	17	17	13	-	193,194,195,196,197, 198,200,201,202,203,204	h57,h58,h59,h60,h61,h64,h65,h66
Cele 315 (CL 315)	14	14	6	14	205,206,207,208, 209,210,211,212,213	h67,h68,h69,h70, h71,h73,h74,h75,h76,
Hetian River (HTR)	8	8	4	-	214,215,216,217,218,219	h77,h78,h79,h80,h81,h82

Table S2 Coordinate point information for SDM analysis of *P. forsythii*.

Species	Longitude (E)	Latitude (N)
P. forsythii	83.12	36.74
P. forsythii	81.57	36.35
P. forsythii	80.75	36.4
P. forsythii	81.16	36.96
P. forsythii	80.02	36.61
P. forsythii	80.37	37.62
P. forsythii	78.1	37.41
P. forsythii	77.25	37.38
P. forsythii	76.16	38.42
P. forsythii	76.49	39.25
P. forsythii	78.95	40.24
P. forsythii	80.29	40.04
P. forsythii	82.57	41.66
P. forsythii	84.3	41.81
P. forsythii	84.2	41.32
P. forsythii	86.56	41.08
P. forsythii	84.27	41.78
P. forsythii	86.07	41.5
P. forsythii	87.85	40.55
P. forsythii	88.35	40.13
P. forsythii	81.9	36.83
P. forsythii	80.81	37.02
P. forsythii	80.02	37.12
P. forsythii	78.22	37.08
P. forsythii	76.77	39.52
P. forsythii	75.87	39.63
P. forsythii	75.94	39.63
P. forsythii	78.45	39.94
P. forsythii	82.67	41.67

Table S3 19 bioclimatic variables.

Name	Bioclimatic variables	Latitude (N)
Bio_1	Annual Mean Temperature	36.74
Bio_2	Mean Diurnal Range (Mean of monthly (max temp - min temp))	36.35
Bio_3	Isothermality (BIO2/BIO7) (* 100)	36.4
Bio_4	Temperature Seasonality (standard deviation *100)	36.96
Bio_5	Max Temperature of Warmest Month	36.61
Bio_6	Min Temperature of Coldest Month	37.62
Bio_7	Temperature Annual Range (BIO5-BIO6)	37.41
Bio_8	Mean Temperature of Wettest Quarter	37.38
Bio_9	Mean Temperature of Driest Quarter	38.42
Bio_10	Mean Temperature of Warmest Quarter	39.25
Bio_11	Mean Temperature of Coldest Quarter	40.24
Bio_12	Annual Precipitation	40.04
Bio_13	Precipitation of Wettest Month	41.66
Bio_14	Precipitation of Driest Month	41.81
Bio_15	Precipitation Seasonality (Coefficient of Variation)	41.32
Bio_16	Precipitation of Wettest Quarter	41.08
Bio_17	Precipitation of Driest Quarter	41.78
Bio_18	Precipitation of Warmest Quarter	41.5
Bio_19	Precipitation of Coldest Quarter	40.55

Table S4 Pair primers used for amplification and sequencing of the mitogenome gene fragment of *P. forsythii*.

Primer name	Sequence(5' to 3')	Annealing temperature
ND2-H	5'- ACATACTCTCGCTTCCAAT -3'	51℃
ND2-L	5'- GTAAATAAACTGATGCCTGC -3'	
ND4-H	5'- CAAACCGAACCCACCTAAT -3'	51℃
ND4-L	5'- AGACCACGGGATTGCTAT -3'	
Cytb-H	5'- CAGCCACCATAGCACATC -3'	53℃
Cytb-L	5'- AGGCGTAGGGAAGAGAAT -3'	

Table S5 The F_{st} among populations of *P. forsythii*.

	HTR	CLL	JS	ALE	LN	YL	RQ	LT	XH	BC	YJS	YC	PS	HT	YT	CL	MF
HTR	0.00000																
CLL	0.08541	0.00000															
JS	0.48300	0.53449	0.00000														
ALE	0.24576	0.11209	0.59191	0.00000													
LN	0.82529	0.78465	0.69904	0.81207	0.00000												
YL	0.76740	0.73730	0.63323	0.77226	0.52157	0.00000											
RQ	0.79069	0.65179	0.63517	0.68886	0.88607	0.84894	0.00000										
LT	0.79353	0.74620	0.63792	0.79031	0.68850	0.61510	0.88408	0.00000									
XH	0.74084	0.60408	0.58931	0.64529	0.87304	0.83093	0.78911	0.86847	0.00000								
BC	0.35737	0.17124	0.57877	0.16799	0.83825	0.79627	0.79758	0.82269	0.76071	0.00000							
YJS	0.94103	0.93150	0.87754	0.95043	0.95606	0.94519	0.96642	0.95052	0.96211	0.95620	0.00000						
YC	0.92951	0.92455	0.88124	0.94106	0.94635	0.93670	0.95069	0.93917	0.94694	0.94373	0.92211	0.00000					
PS	0.90266	0.90527	0.86572	0.92430	0.92899	0.91735	0.92729	0.91680	0.92299	0.92276	0.89472	0.75894	0.00000				
HT	0.94098	0.93411	0.89443	0.94867	0.95293	0.94437	0.95959	0.94675	0.95649	0.95233	0.93593	0.90369	0.87849	0.00000			
YT	0.73572	0.78046	0.73969	0.81942	0.82126	0.79908	0.78651	0.78103	0.77690	0.79559	0.73744	0.57189	0.28471	0.60699	0.00000		
CL	0.96724	0.95067	0.91037	0.96184	0.96790	0.96047	0.98064	0.96727	0.97892	0.97031	0.95728	0.87738	0.48232	0.93874	0.24472	0.00000	
MF	0.98497	0.97466	0.95132	0.98104	0.98437	0.98077	0.99221	0.98497	0.99131	0.98608	0.98177	0.97463	0.96311	0.97845	0.89515	0.98846	0.00000

Table S6 Estimates of gene flow (the 95% confidence intervals are given in brackets) and theta between regional groups of *P. forsythii*.

Source group	Theta (2Neμ)	Values of 2Neμ for each recipient group								
		Group 1	Group 2	Group 3	Group 4	Group 5	Group 6	Group 7	Group 8	Group 9
Group 1	0.02572		261.78	241.42	484.56	23.99	454.78	1.6	0.63	3.82
Group 2	0.0017	396.48		185.81	215.72	12.95	608.82	9.25	2.26	1.08
Group 3	0.00098	88.09	195.07		262.88	46.45	71.44	6.83	3.39	1.75
Group 4	0.00212	302.16	294.05	158.48		16.01	301.41	7.28	3.78	2.33
Group 5	0.00354	43.2	26.34	391.7	17.17		71.03	7.17	1.34	1.75
Group 6	0.00242	468.81	426.43	134.6	72.55	25.11		5.48	0	2.97
Group 7	0.0013	1.25	0	0	0	0	0		0	3.52
Group 8	0.02006	0	10.69	0	0	2.15	2.35	11.42		7.11
Group 9	0.00096	0	0	0	0	0	1.96	0	0	

Note: Group 1: MF; Group 2: HT, YT, YC, PS, CL; Group 3: YJS; Group 4: BC, XH, ALE; Group 5: LN, LT; Group 6: JS; Group 7: YL; Group 8: RQ; Group 9: HTR, CL315